ORIGINAL RESEARCH ARTICLE

Reef island evolution in a turbid-water coral reef province of the Indo-Pacific

Joshua L. Bonesso[1,2,3,4] | Michael V. W. Cuttler[3,5] | Nicola K. Browne[6,7] | Caroline C. Mather[8] | Victorien Paumard[1,3,9] | William T. Hiscock[10,11] | John N. Callow[3,12] | Michael O'Leary[1,3,9]

[1]School of Earth Sciences, University of Western Australia, Perth, Western Australia, Australia

[2]ARC Centre of Excellence for Coral Reef Studies, University of Western Australia, Perth, Western Australia, Australia

[3]UWA Oceans Institute, University of Western Australia, Perth, Western Australia, Australia

[4]Western Australian Marine Science Institution, Perth, Western Australia, Australia

[5]Oceans Graduate School, University of Western Australia, Perth, Western Australia, Australia

[6]School of Life and Molecular Sciences, Curtin University, Perth, Western Australia, Australia

[7]School of Biological Sciences, University of Queensland, Brisbane, Queensland, Australia

[8]Centre for Rock Art Research and Management, School of Social Sciences, University of Western Australia, Perth, Western Australia, Australia

[9]Centre for Energy and Climate Geoscience, University of Western Australia, Perth, Western Australia, Australia

[10]Earth and Sustainability Science Research Centre, School of Biological, Earth and Environmental Sciences, University of New South Wales, Sydney, New South Wales, Australia

[11]Chronos [14]Carbon Cycle Facility, Mark Wainwright Analytical Centre, University of New South Wales, Sydney, New South Wales, Australia

[12]UWA School of Agriculture and Environment, University of Western Australia, Perth, Western Australia, Australia

Correspondence
Joshua L. Bonesso, School of Earth Sciences, University of Western Australia, Perth, WA 6009, Australia.
Email: joshua.bonesso@research.uwa.edu.au

Abstract

Coral reef islands are vulnerable landforms to environmental change. Constructed of largely unconsolidated reef-derived sediments, they are highly sensitive to variations in metocean boundary conditions, raising global concern about their future resilience and stability in the face of increased natural hazards, sea-level rise and anthropogenic climate change. This study examines the evolution of an inshore turbid reef island from the southern Pilbara region of Western Australia (Indo-Pacific) using detailed analyses of island chronostratigraphy (composition, texture) and geochronology (21 *in-situ* radiometric dates) from Eva Island. Downcore, composition of island-grade (reef-derived) sediments were homogenous, dominated by molluscan (37%–42%) and coral (32%–37%) constituents. The ^{14}C radiometric dating of island sediments, beachrock and coral microatolls identified five stages of island formation across changing sea-level regimes over the mid to late Holocene: (1) limestone platform accretion at *ca* 6,000 cal yr BP, coinciding with reef decline or 'give-up' on neighbouring Exmouth Gulf reefs; (2) sand cay (i.e. core) initiation and vertical aggregation at *ca* 5,000 cal yr BP during

the point of sea-level regression to current levels; (3) major accretion and lateral progradation of the island between 3,500 cal yr BP and 2,500 cal yr BP including the modification of island shorelines through alongshore reworking of sediment; (4) lateral accretion and minor expansion to the north and formation of beachrock pavement between 2,500 and 650 cal yr BP; and (5) planform adjustment (erosion of the north-west island) and backstepping under stabilised sea levels over the past 650 years. While this model is comparative to studies on island formation following incremental sea-level fall following the mid-Holocene highstand, it demonstrates active landform readjustment under stabilised sea levels over the past 2,000 years, probably the influence of local-scale metocean boundary conditions within climate windows across the mid to late Holocene period (i.e. independent of sea-level fluctuations). Importantly, while sediment production rates are predicted to be lower in turbid-water reef systems than clear water, Eva Island shows no change in carbonate producers (i.e. proportion of mollusc and coral) over the course of island building, indicating the carbonate factory has not experienced significant adjustments in reef ecology, but has remained stable despite low water quality.

1 | INTRODUCTION

Coral reef islands are low-lying sedimentary landforms that form atop reef platforms or atoll rims. Reef-derived biogenic sediments constitute the dominant island grain type, which are transported lagoonward through waves and currents, and accumulate as hydrodynamic energy begins to dissipate (Dawson et al., 2012; Ford et al., 2020; Perry et al., 2011; Yamano et al., 2014). The biogenic sediments that comprise reef islands are predominantly derived from their adjacent coral reefs and consist of the skeletal remains of calcifying reef biota such as coral, crustose coralline algae (CCA), molluscs, foraminifera, echinoids and *Halimeda* (Bonesso et al., 2022; Kench et al., 2005; Liang et al., 2022; Woodroffe, 1992; Yamano et al., 2000). Reef islands provide a habitable landform for coastal island nations (e.g. atoll nations) and endemic/threatened flora and fauna (e.g. sea turtles, sea/shorebirds), however, they are highly vulnerable to projected climate change impacts, particularly sea-level rise (SLR) and changing wave climate. These threats may increase the risk of landform destabilisation and erosion, rendering them uninhabitable (East et al., 2018; Ford et al., 2020; Storlazzi et al., 2018).

Globally, numerous studies have established the onset and development of reef islands over the last *ca* 6,000 cal yr BP, with sea-level fall during the mid to late Holocene considered as the critical driver (Dickinson, 2009; Ford

et al., 2020; Liang et al., 2022). Reinforcing this island development model is the precondition that the reef platform, or lagoon infill has reached sea level before island accretion can initiate. For example, reconstructions of island evolution from the Indian Ocean (e.g. Cocos [Keeling] Islands; Maldives Archipelago), Pacific Ocean (e.g. Kiribati, Central Pacific) and Torres Strait (e.g. Bewick Cay, Great Barrier Reef), demonstrate that island construction initiated following the mid-Holocene highstand (i.e. into the Holocene regression), the point at which accommodation space for vertical coral reef growth becomes constrained in response to a fall in sea level (Kench et al., 2012; Woodroffe et al., 1999; Woodroffe & Morrison, 2001). However, emerging geological evidence from the south-west Pacific (e.g. Jabat Island, Marshall Islands) and eastern Indian Ocean (e.g. Maldives Archipelago) suggest island formation has occurred prior to (i.e. latter stages of Holocene SLR; Kench et al., 2005) and during the mid-Holocene highstand (East et al., 2018; Kench et al., 2014). Collectively, these studies reinforce the variability in island building processes and local effects, demonstrating formation under a variety of sea-level scenarios and reef growth (or lagoon infill) histories (Kench et al., 2020).

This study examines, for the first time, island building processes of an inshore turbid-water reef island located within Exmouth Gulf in the southern Pilbara region of Western Australia, using a combination of (1)

chronostratigraphic and (2) accelerator mass spectrometry (AMS) ^{14}C radiocarbon age dating analyses. Unlike global reef island counterparts (e.g. Maldives Archipelago), the Pilbara inshore islands are situated within a region of high spatial and temporal variability in turbidity, fringed by shallow turbid coral reefs and exhibit landmass elevations to and exceeding 18 m above mean sea level (amsl) and volumes of 4.7 million m^3 (e.g. Long Island; Bonesso et al., 2020). While prior research has focussed on island building within clear-water (oligotrophic) coral reef settings, no previous studies have reconstructed island development within turbid-water reef ecosystems, highlighting a critical knowledge gap. Turbid-water systems are sensitive and have been typically synonymous with lower carbonate production rates compared to clear-water systems. Yet, as clear-water coral reefs trend towards these environments with climate change (Cacciapaglia & van Woesik, 2015; Heery et al., 2018; Zweifler et al., 2021), it is important to understand turbid systems and the implications for reef island development. An improved understanding of contemporary turbid-water systems may, therefore, help enhance future management of present-day clear-water systems and their island landforms under future perturbations in environmental conditions. Thus, this study provides the first detailed reconstruction of reef island evolution in Western Australia, and insights into the onset and timeframes of island formation in a turbid-water reef province of Australia, and more broadly, the Indo-Pacific region.

2 | STUDY SITE—REEF ISLAND MORPHOLOGY, CLIMATE AND OCEANOGRAPHIC CONDITIONS

Island accretion and evolution was examined for Eva Island (21°55′19″ S, 114°25′55″ E), an inshore sand cay located in the Exmouth Gulf, at the southern extent of the Pilbara region, Western Australia (Figure 1A through D). The island planform shape is roughly circular with a total area of 14.7 ha (0.147 km^2), volume of 559,427 m^3, and a maximum elevation of 8.6 m above sea level (Bonesso et al., 2020). Island geomorphology is characterised by a mobile spit, vegetated foredunes (i.e. low-lying vegetation [*Spinifex sericeus*] <1 m in height) and a central basin/depression. Remnant underlying beachrock is present on the north-northwestern periphery and extending off the southern edge of the landmass (i.e. historical island footprint; Figure 2A through F). Surficial sediments collected from the island landmass (beach, foredunes, central basin) and adjacent limestone reef platform/sub-reef environments indicate that Eva Island and reef is composed of unconsolidated biogenic carbonate fragments rich in mollusc

(34% of reef and island sediments, respectively) and coral constituents (31% of reef and 27% of island; see Bonesso et al., 2022).

The North West Cape region of Western Australia's Pilbara region has a dry arid climate, with very hot humid summers (average temperature between 36 and 37°C from November to April) and cool mild winters (average temperature between 28 and 29°C from May to October). Rainfall is low (*ca* 260 mm/year), commonly associated with tropical cyclone/tropical low activity during the first 6 months of the year (with approximately three tropical cyclones annually within the Exmouth region) (Cartwright et al., 2021; Cuttler et al., 2020). The semi-enclosed waters of the Exmouth Gulf experience a semi-diurnal tidal regime, with an average tidal range of 1.8 m. The Gulf experiences seasonal and inter-annual variability in wind and wave regimes influenced by: (1) long period wave energy (peak period *ca* 7–10 s) ocean swell waves that propagate into the Gulf from the north-northwest during the Austral winter, and (2) short period, locally generated wind–waves (peak period *ca* 5 s) from the south-southwest during the Austral summer (Cuttler et al., 2020). These factors, in addition to south-west flowing tidal currents (Dufois et al., 2017), increase sediment resuspension and result in high spatial and temporal turbidity throughout the year, with mean monthly turbidity (Total Suspended Material, TSM) ranging between 0.75 and 5.7 mg/L (Cartwright et al., 2021). Seasonally, turbidity patterns in the Gulf are higher during the winter (coinciding with the intensification of easterly trade winds and swell waves), with TSM fluctuating between 1 and 2 mg/L at Eva Island (Cartwright et al., 2021).

3 | SAMPLING AND ANALYTICAL METHODS

3.1 | Core recovery, logging and analysis

Four sediment cores (hereafter: PC2–PC5) were collected at Eva Island using a manual sand auger in October 2021, recovered at 20 cm intervals to a maximum depth of approximately 5 m below the island landmass surface (i.e. foredune ridge, island basin; Figure 3). Following collection, 100 g of sediment was sub-sampled from each 20 cm interval along the four cores PC2–PC5 ($n = 95$ samples, total) for composition (i.e. biogenic and siliciclastic) and grain-size analyses (i.e. mean grain size [μm] and sorting [σ]). All sediment samples were rinsed in freshwater and dried at 60°C for 48 h prior to processing and laboratory analyses. Standard wet sieving protocol was performed to separate the samples into seven fraction sizes (>4,000, 2,000, 1,000, 500, 250, 125 and 63 μm) in accordance with methodology outlined
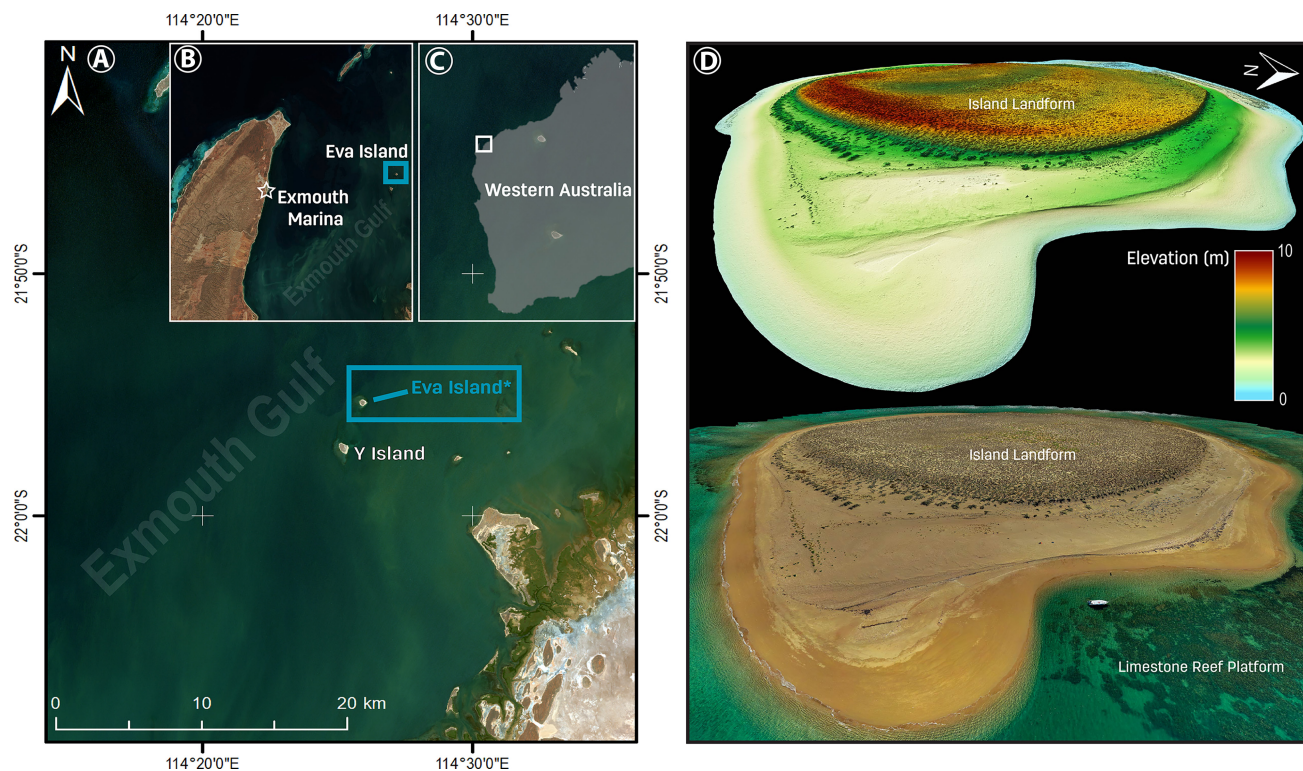
FIGURE 1 Location of (A) study site Eva Island (highlighted in blue) and location within the Exmouth Gulf; (B) Exmouth Marina (white star) in the western Exmouth Gulf (C) Exmouth Gulf Region in Western Australia and (D) 3D Digital Elevation Model (DEM) model (top) and drone photograph (below) of Eva Island. Photogrammetry data to create orthophoto mosaics (1.9 cm) and Digital Elevation Model (DEM, 3.3 cm) was collected over Eva Island in November 2021 using a Remotely Piloted Aircraft (RPA, Phantom 4 RTK). Data were processed in Agisoft Metashape© (Callow et al., 2018; May et al., 2017, 2021) and the resulting DEM and orthomosaic were exported to Fledermaus© (Quality Positioning Services, QPS), with the orthomosaic draped over the DEM to allow 3D visualisation of the island and adjacent reef flat. The photogrammetry derived DEM was used for qualitative observation only (see Supplementary Material for full details on drone imagery processing for Figure 1D).

in Bonesso et al. (2022). Sediment texture (average grain [µm] size and sorting [σ]) was calculated in GRADISTAT© (Blott & Pye, 2001; Table 1). Biogenic and siliciclastic composition of the 95 sediment samples was determined using randomised point counts under a Nikon SMZ445 binocular microscope (Belgium Metrology©, Belgium) by identifying a minimum of 200 grains per sample from the 1,000 and 500 µm fractions. These two size fractions were chosen for identification as they represented the dominant sand-grade material (by % mass). Sediment was classified into the following categories: coral, molluscs (univalve gastropods and disarticulated bivalves), echinoderms, CCA, foraminifera, bryozoans, *Halimeda*, siliciclastic (quartz), limestone, other reefal calcifier (i.e. crustaceans and sponge/coral spicules) and unknown.

Site PC1 is an exposed foredune on the north-west periphery of the landmass (i.e. exposed cross-section exhibiting depositional sequences) from which only pristine mollusc constituents were sampled for AMS ^{14}C radiocarbon age dating (Figure 3). No sediment textural or compositional analyses were performed for PC1.

3.2 | Radiocarbon (^{14}C) age dating of coral microatoll, beachrock and island sediments

To ascertain relative timing of island accretion and evolution, ^{14}C radiocarbon age dating was employed for reef-derived sediments (Ford et al., 2020) using AMS at

FIGURE 2 Geomorphic observation during field work at Eva Island showing; (A) aerial view of island landmass; (B) manual sand auguring to extract cores within island basin; (C) exposed beachrock pavement at the northern periphery of island landmass; (D) coring of fossil coral microatoll (*Porites* sp.) on northern limestone platform of island; (E) scarped foredune (with coastal spinifex grass) and location of core PC1 and (F) aerial view of scarped foredune, beachrock pavement, limestone platform, patch reef and reef crest zones. Aerial drone photography was performed using a DJI Phantom 4 RTK, flying at a maximum altitude of 120 m in October 2021.
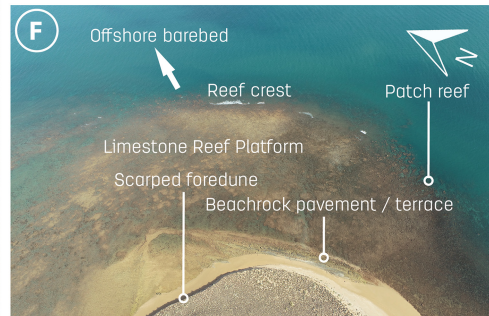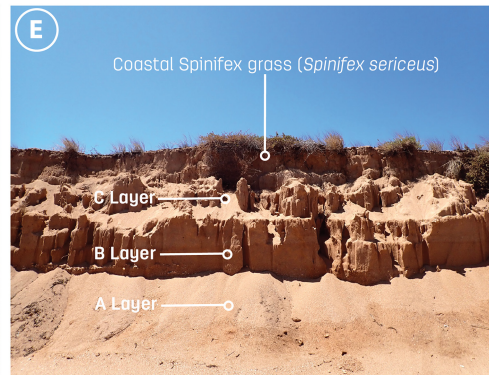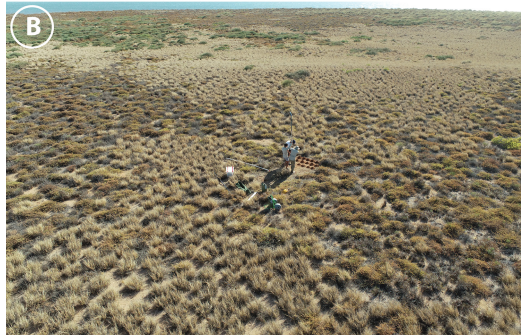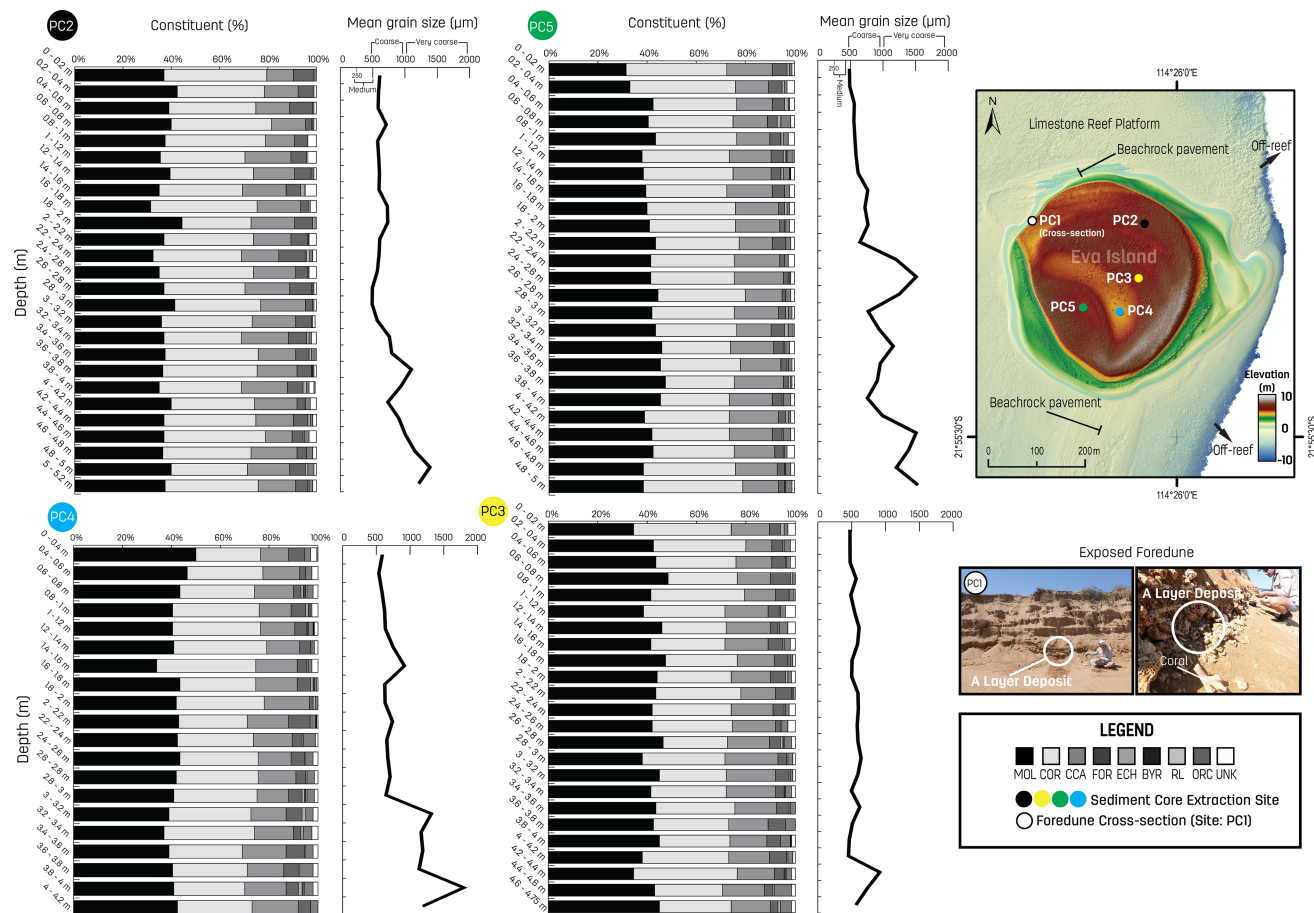
FIGURE 3 Percentage (%) of reef-derived constituents downcore for island cores PC2–PC5. Core locations are shown overlaid on airborne-bathymetric LiDAR DEM of Eva Island (0.5 m resolution, derived from Bonesso et al., 2020).

TABLE 1 Summary of island core sediment composition (skeletal) and texture (grain size, sorting) from Eva Island.

Core ID	Skeletal Composition (%)				Sediment Texture			
	Coral	Mollusc	CCA	Foraminifera	Grain size range (μm)	Average grain size (μm)	Sorting range (μm)	Average sorting (μm)
PC2	36.8 ± 3.6	37.5 ± 2.8	16.3 ± 2.4	6.0 ± 2.0	490–1387	756.3 ± 240.9	1.48–2.48	1.75 ± 0.21
PC3	31.8 ± 4.2	42.4 ± 3.6	16.2 ± 2.4	4.9 ± 1.4	452–914	565.4 ± 100.5	1.54–2.56	1.78 ± 0.28
PC4	32.7 ± 3.5	41.6 ± 3.2	15.5 ± 2.0	4.9 ± 1.7	536–1797	854.3 ± 334.5	1.51–2.59	1.99 ± 0.29
PC5	34.3 ± 3.6	41.1 ± 3.7	16.6 ± 2.1	3.6 ± 1.3	485–1535	860.6 ± 341.4	1.59–2.94	2.11 ± 0.42

Note: CCA is synonymous for Crustose Coraline Algae. Average composition (% ± SD) of reefal constituents are reported alongside both mean grain size (μm ± SD) and sediment sorting values (μm ± SD). Range of grain size and sorting are denoted as the minimum and maximum values across each core (PC2–PC5).

the Chronos [14]Carbon-Cycle Facility (Mark Wainwright Analytical Centre), University of New South Wales (UNSW), Sydney, Australia. A total of 21 samples were obtained from island sediment, beachrock and coral microatolls (*Porites* sp.), including 12 intact gastropod shells from sediment cores (Code: PC), three shell fragments extracted from exposed beachrock deposit (Code: BR), three fossil coral microatoll specimens (Code: CO, *Porites* sp.) and

three intact bivalve shells from the exposed island foredune deposit (Code: E_NW). To ensure accurate and robust ^{14}C radiocarbon ages are obtained, the most pristine, intact and least durable reefal constituents were selected to minimise the effects of the lag between death and deposition with low likelihood of alteration during storage and/or transport prior to deposition (Kench et al., 2011). Details of the sample type and depth relative to MSL are shown in Table 2.

TABLE 2 Summary of sample information and radiocarbon (^{14}C) ages including the conventional age, 1σ range of calibrated age and calibrated age with median probability.

Lab code	Sample code	Material type	Elevation relative to MSL (m)	1σ range of conventional age (yr BP)	1σ range of calibrated age (cal yr BP[a])	Calibrated age with median probability (cal yr BP[a])
UNSW-1414	E_PC_02A	Sediment core (intact gastropod)	3.2–3.4	1899 ± 32	1230–1510	1370
UNSW-1415	E_PC_02B	Sediment core (intact gastropod)	4.2–4.4	2247 ± 32	1583–1909	1746
UNSW-1416	E_PC_02C	Sediment core (intact gastropod)	5–5.2	2299 ± 33	1647–1979	1813
UNSW-1417	E_PC_03A	Sediment core (intact gastropod)	3.2–3.4	3214 ± 36	2758–3101	2929
UNSW-1418	E_PC_03B	Sediment core (intact gastropod)	4–4.2	3067 ± 34	2611–2925	2768
UNSW-1419	E_PC_03C	Sediment core (intact gastropod)	4.6–4.75	4741 ± 37	4678–5064	4871
UNSW-1420	E_PC_04A	Sediment core (intact gastropod)	1–1.2	3581 ± 35	3221–3546	3383
UNSW-1421	E_PC_04B	Sediment core (intact gastropod)	2.6–2.8	2840 ± 34	2333–2676	2504
UNSW-1422	E_PC_04C	Sediment core (intact gastropod)	4.0–4.2	3451 ± 36	3055–3389	3222
UNSW-1423	E_PC_05A	Sediment core (intact gastropod)	2–2.2	3604 ± 36	3243–3571	3407
UNSW-1424	E_PC_05B	Sediment core (intact gastropod)	3.4–3.6	3541 ± 36	3165–3489	3327
UNSW-1425	E_PC_05C	Sediment core (intact gastropod)	4.8–5	3101 ± 35	2665–2959	2812
UNSW-1426	E_NW_AL	Foredune (intact bivalve)	3.0–3.2	1317 ± 32	645–905	775
UNSW-1427	E_NW_BL	Foredune (intact bivalve)	2.2–2.4	1301 ± 32	633–898	765
UNSW-1428	E_NW_CL	Foredune (intact bivalve)	1.0–1.2	1301 ± 32	534–788	661
UNSW-1430	BR_W_01	Beachrock (disarticulated gastropod)	0.5	2866 ± 35	2350–2694	2522
UNSW-1431	BR_W_02	Beachrock (disarticulated gastropod)	0.5	1589 ± 32	898–1192	1045
UNSW-1432	BR_W_03	Beachrock (disarticulated gastropod)	0.5	2060 ± 34	1374–1688	1531
UNSW-1433	C02	Coral microatoll (*Porites* sp.).	−0.4	5011 ± 39	5015–5423	5219
UNSW-1434	C02a	Coral microatoll (*Porites* sp.)	−0.4	5658 ± 42	5737–6116	5926
UNSW-1435	C04	Coral microatoll (*Porites* sp.)	−0.3	4258 ± 48	4042–4452	4250

[a]^{14}C results calibrated using OxCal© v4.4.4 and ΔR of −61 ± 14 years.

Samples were pre-treated following the protocols outlined for carbonates in Turney et al. (2021). To remove any surface contamination, samples were cleaned by physical abrasion and prolonged sonication in distilled water and then surfaces were etched with 0.1 M HCl to remove the outer layer of the sample, before being rinsed with ethanol and oven-dried at 70°C (Turney et al., 2021). Samples were pulverised with a vibratory mill in a tungsten carbide grinding bowl with a single disc. Pre-treated samples were converted to CO_2 by reaction with 85% H_2PO_4 (1 mL 85% v/v) at 40°C and flushed through a phosphorus pentoxide (Merck SICAPENT®) trap with helium gas to be transferred into the AGE3 system (Ionplus®, Switzerland) (Turney et al., 2021; Wacker et al., 2010). The CO_2 was concentrated in a zeolite trap, heated to 420°C and released as pure CO_2 into the graphitisation reactor tube where it was reduced to graphite over an iron catalyst at 580°C within the AGE3 system (Turney et al., 2021; Wacker et al., 2010). Radiocarbon (^{14}C) measurement was carried out using a MICADAS (Ionplus®, Switzerland) accelerator mass spectrometer (Wacker et al., 2010), following sample measurement procedures outlined by Turney et al. (2021). The ^{14}C results are reported as calendar years before present (hereafter: cal yr BP) following correction for the reservoir age. The ages were calibrated using the online software OxCal© v4.4.4 (Ramsey, 1995), the Marine20 calibration curve (Heaton et al., 2020) and the local marine reservoir effect (ΔR) for the region (around Exmouth Gulf) of −61 ± 14 years.

4 | RESULTS

4.1 | Sediment texture and composition of reef island cores

Medium to very coarse sand (250–2,000 μm) dominated all four island core samples (PC2–PC5, 94.8%, on average) with gravels and silt-sized material accounting for 4.2% and 0.9% respectively (Figure 3). Downcore

variation was observed across the island cores, with upper island units generally consisting of medium sands, from which coarse and very coarse sand layers occur with increasing depth from the surface (452–1,797 µm range across all cores). Sorting (µm) decreased downcore, with moderately well-sorted upper units and poorly sorted lower units (1.48–2.94 µm range across all cores). Skeletal composition of island sediments was homogenous downcore (i.e. no variation between upper and lower sedimentary units) and was dominated by mollusc (37%–42%) and coral (32%–37%) with subordinate fractions of CCA (16%) and foraminifera (4%–6%; Table 1).

4.2 | Radiocarbon ages of coral microatoll, beachrock and island sediments

4.2.1 | Coral microatolls and beachrock ages

Calibrated ^{14}C ages of coral microatolls (Code: CO, $n = 3$, *Porites* sp.) on the north-west and west limestone platform of Eva Island yielded an age range of 4,250–5,926 cal yr BP, which included the oldest set of ages across all collected samples (Figure 4A; Table 2). Dating of disarticulated shell fragments from exposed beachrock pavement (Code: BR, $n = 3$) fringing the north-northwest periphery of the island landmass recorded an age range of 1,045–2,522 cal yr BP (Figure 4A).

4.2.2 | Island sediment ages

Along Profile 2 (Code: P2) of the island landmass, the oldest date on intact gastropod clasts is located at the base of sediment core PC3 (Depth: 4.6–4.75 m) with an age of 4,871 cal yr BP (Table 2 and Figure 4C). Dating of gastropod clasts at 3.2–3.4 m and 4–4.2 m depth from PC3 show a 2,000-year time lag in deposition, recording ages of 2,929–2,768 cal yr BP respectively. An age determination of 3,222 cal yr BP was recorded at the base of sediment core PC4 (Depth: 4–4.2 m), followed by an age inversion at a depth of 2.6–2.8 m and 1–1.2 m, with sediment clasts dating at 2,504–3,383 cal yr BP respectively. Sediment core PC5 also showed evidence of age inversion across the core profile, with the youngest age determination at the base recorded at 2,812 cal yr BP (Depth: 4.8–5 m), followed by 3,327–3,407 cal yr BP at a depth of 3.4–3.6 m and 2–2.2 m, respectively. In summary, age determinations across PC3, PC4 and PC5 are suggestive of deposition between 5,000 and 2,500 cal yr BP (Table 2 and Figure 4C).

Gastropod clasts extracted from PC2 on the northern periphery of the landmass recorded radiometric ages between 1,813 cal yr BP (Base of core, 5–5.2 m) and 1,370 cal yr BP (Depth: 3.2–3.4 m). Notably, no chronostratigraphic age inversion was evident. PC1, located at the exposed foredune (Location NW, Profile 1, Figure 4B) recorded the youngest radiometric (^{14}C) ages, ranging between 775 cal yr BP (Depth: 3–3.2 m depth) and 661 cal yr BP (Depth: 1–1.2 m depth).

5 | DISCUSSION

Five conceptual phases of reef island development have been identified based on a combination of sedimentological, geomorphological and geochronological datasets for the inshore sand cay Eva Island, in the southern Pilbara region of Western Australia, Indo-Pacific.

5.1 | Phase 1: Scenario of reef accretion of Eva reef flat and context within the Exmouth Gulf, Western Australia

There are limited island reef core data from the Exmouth Gulf that can determine when reef flats/limestone reef platforms became established and thus provide the foundation for island development. Yet, insights from neighbouring fringing reefs along the Exmouth Gulf's western coast may be used to infer this record (Figures 5A and 6A). A reef growth study by Twiggs and Collins (2010) off the Exmouth Marina (Figure 1B) shows reef development had initiated in Exmouth Gulf by at least 7,500 cal yr BP, coinciding with the onset of the Holocene highstand, with the reef continuing to aggrade vertically until around 6,500 cal yr BP. Between 6,500 and 5,800 cal yr BP the reefs are postulated to have entered 'give up' mode due to a lack of accommodation space when sea-levels stabilised across the mid-Holocene highstand and began to fall by the end of this stage (SL at 5,800 cal yr BP = 2 m; Twiggs & Collins, 2010). To place the development of Eva Island's reef into context, comparison has been made with a composite Holocene sea-level curve developed by Twiggs and Collins (2010). On the limestone reef platform at Eva Island, the oldest coral fossil microatoll (*Porites* sp.) was measured at 5,926 cal yr BP (*ca* 6,000 cal yr BP; Figure 4A), coinciding with the stage of reef decline or 'give-up' on the Exmouth Gulf's west coast (Twiggs & Collins, 2010). The elevation of the *Porites* microatoll is −0.40 m relative to present MSL (Table 1), which is 1.6–2.1 m above the surveyed height of living *Porites* from the 'live coral patch reef' at the edge of the limestone platform (mean elevation range sourced from Bonesso et al., 2022). The age determination and elevation of the coral microatolls on Eva suggest the limestone
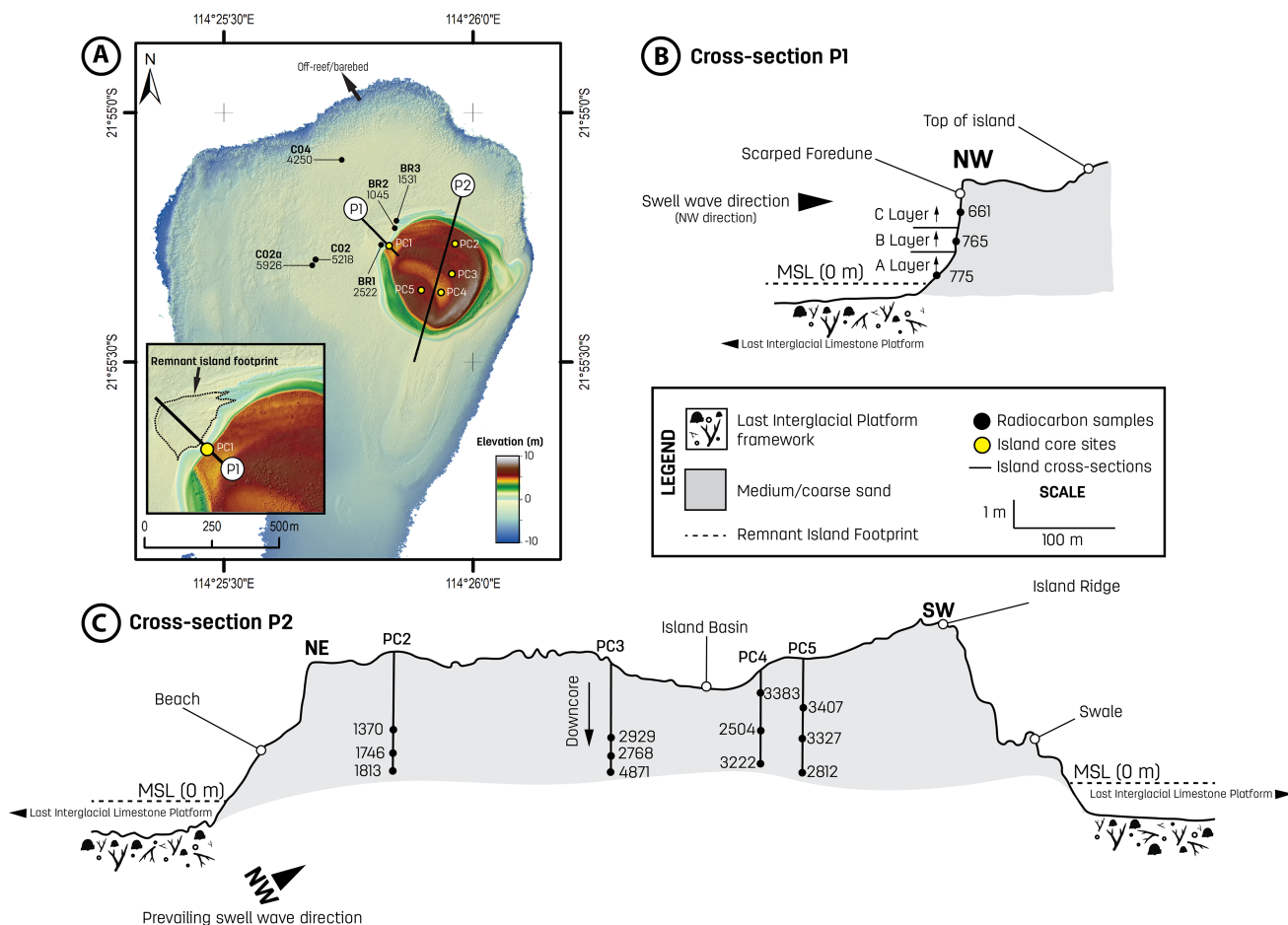
FIGURE 4 (A) Island core locations (yellow dots), radiocarbon sample sites (black dots), and region of remnant island footprint as shown on airborne-bathymetric LiDAR DEM of Eva Island (0.5 m resolution, derived from Bonesso et al., 2020); (B) island cross-section along Profile 1 (P1) showing radiocarbon sample ages (black dots) for PC1 core on NW periphery of island landmass and (C) island cross-section along Profile 2 (P2) showing radiocarbon sample ages (black dots) for cores PC2–PC5.

reef platform had established by at least 6,000 cal yr BP and subsequently became emergent as sea-levels fell; therefore, island development on Eva's platform could have initiated by 6,000 cal yr BP.

5.2 | Phase 2: Island core initiation and vertical aggradation

The formation of Eva Island as a sand cay had initiated by 4,871 cal yr BP on the eastern side of the limestone reef platform (Figures 4C, 5B and 6B). Significantly, Holocene sea level had begun to regress and stabilise to current levels during this phase (Collins et al., 2006; Twiggs & Collins, 2010). Notably, sediments during this preliminary stage of island core formation are characterised by poorly sorted coarse sands rich in mollusc/coral constituents, probably sourced from the surrounding limestone reef platform and delivered to the island core by the focussing effect of local hydrodynamic processes (Gourlay 1988).

5.3 | Phase 3: Sustained island accretion and planform adjustment

Sustained accretion between 3,500 and 2,500 cal yr BP allowed lateral progradation of Eva Island, which established much of the island landmass (Figures 4C, 5C and 6C). Across this 1,000-year window (post-island core formation) sediment composition of the mid and upper island units remain dominated by mollusc and coral constituents, reflecting no apparent or significant ecological adjustments as a result of relative sea-level fall (i.e. a fall in sea level was not fatal for limestone reef platform biota). After 2,500 cal yr BP, there is evidence that Eva Island probably underwent planform adjustment, with date inversion at PC5 suggestive of the reworking of an existing reservoir of island sediments. According to Liang et al. (2022), date inversion may be indicative of active reworking of island-grade material through a combination of alongshore flux and recirculation, particularly on an island's lateral margins. At Eva
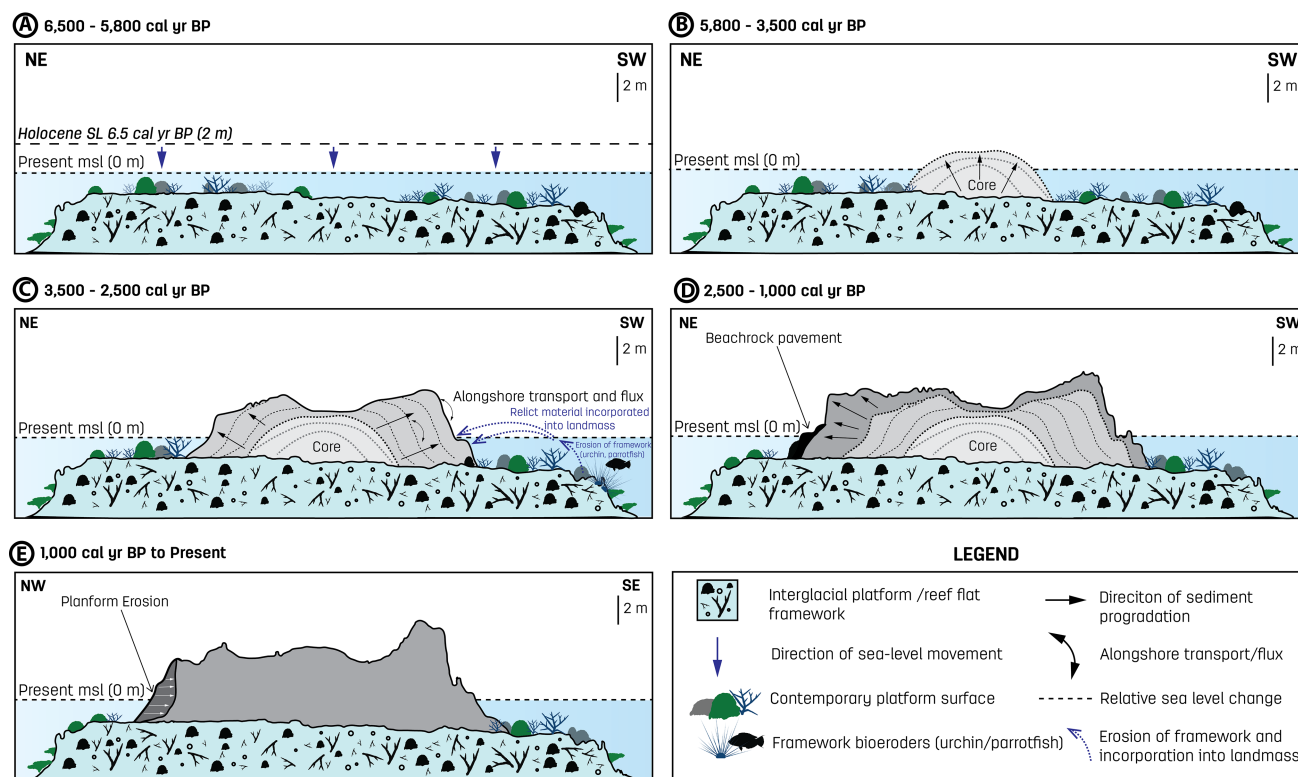
FIGURE 5 Cross-section schematic model for the accretion of Eva Island, Pilbara region of Western Australia (Indo-Pacific) over the past 6,500 cal yr BP.

Island, this reworking of material may have been caused by local wind-wave regimes, whereby prevailing wind-generated waves from the south-southwest, coupled with potential pulse high energy events (i.e. historical tropical cyclones; Nott, 2011) resulted in shoreline adjustment and recirculation of island sediments across the then present shoreline (Cuttler et al., 2020; Wu et al., 2021a). Alternatively, bioerosion (e.g. sea urchin, serpulids, parrotfish) and mechanical erosion (i.e. increased wave exposure) of the limestone reef platform (as sea-level fell) may have released sediment that was previously (at higher sea levels) incorporated into the reef framework (Cuttler et al., 2019). This older 'relict' material could then have been reconstituted and transported towards the beach, deposited on top of contemporary sediments already deposited on the island shoreline, resulting in older radiocarbon ages overlain atop of younger.

5.4 | Phase 4: Stable accretion and lateral progradation towards the north

Over a 1,000-year window from 2,000 cal yr BP, Eva Island began to laterally prograde northward, through stable incremental accretion (Figures 5D and 6D). Sequence stratigraphy of radiocarbon ages between 1,813 and 1,370 cal

yr BP (Accretion event at core PC2; Figures 4C, 5D and 6D) are suggestive of little to no planform adjustment or extensive sediment reworking across this timeframe. In addition, geomorphic stability during this period is reinforced by the formation of beachrock pavement (Liang et al., 2022; Vousdoukas et al., 2007) along the northern sectors of the island shoreline between 2,500 and 1,000 cal yr BP. A latter sequence of island accretion is characterised by the limited progradation of the island margin to the north-northwest between 1,000 and 650 cal yr BP (Accretion event at core PC1; Figures 4B, 5D and 6D). Exposed foredune stratigraphy at core location PC1 at Eva's north-west margin, indicate subtle geomorphic change, with the youngest recorded radiometric age dates ranging from 775 to 661 cal yr BP (Figures 4B and 5D).

5.5 | Phase 5: Planform adjustment under stabilised sea levels

At a timepoint between 650 cal yr BP and the current day, the north-west sector of the island underwent erosional scarping, undercutting the north-west foredune, and back-stepping to its present position (Figures 5E and 6E; Bonesso et al., 2020). Contemporary erosion is evident via the scarped foredunes with a >30° angle of repose (i.e. an identified erosional signature; see Bonesso et al., 2020). Yet, a remnant
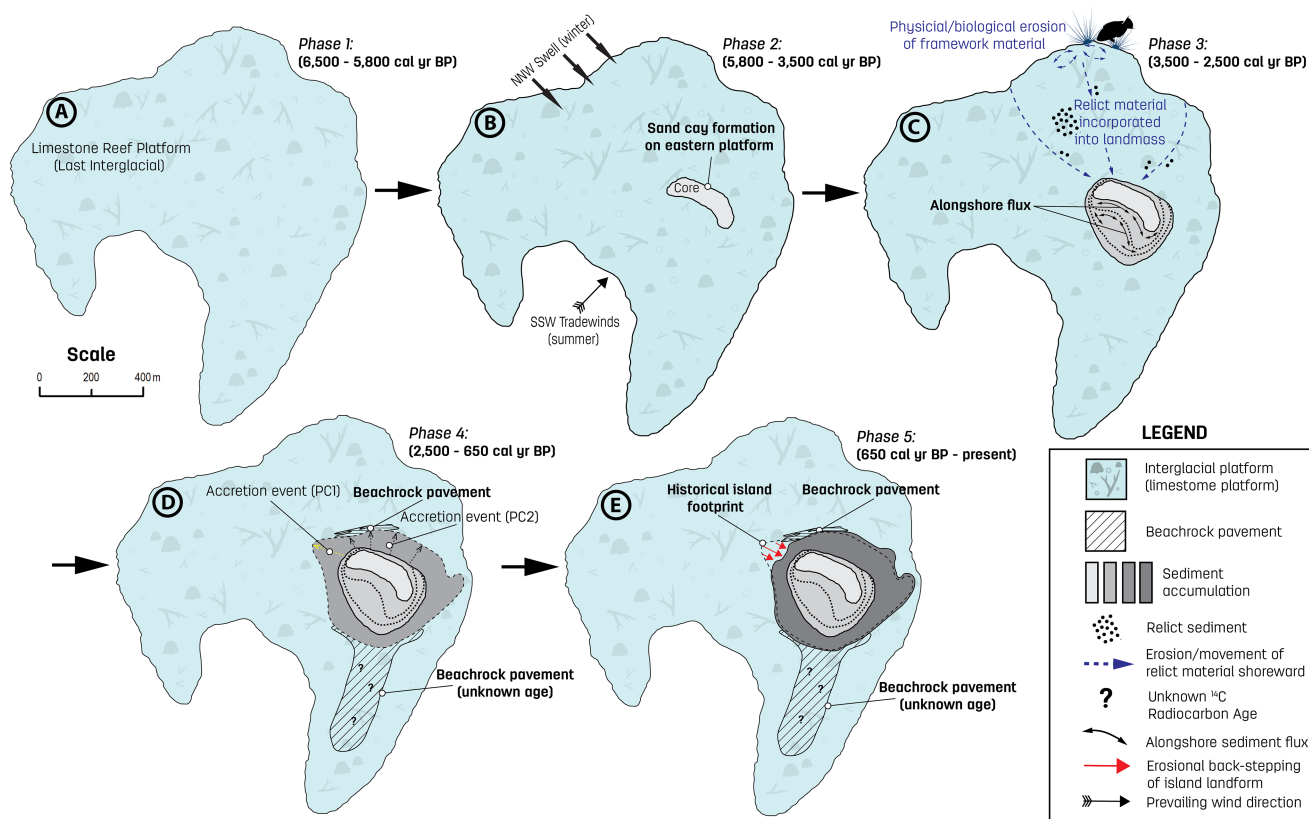
FIGURE 6 Aerial schematic model for the accretion of Eva Island, Pilbara region of Western Australia (Indo-Pacific) over the past 6,500 cal yr BP.

island footprint (observed on the LiDAR DEM; Figure 4A) is visible, suggesting that the foredune was progressively eroded back over time to its present position within the last 650 years. This may have been the result of changes in sediment supply (i.e. sediment deficit) from that side and/or changes in physical forcing (wind/wave regimes) over this climate window (Cuttler et al., 2020; Wu et al., 2021b).

5.6 | Eva Island in the context of global reef island evolution models

The model of evolution at Eva Island reports reef island building processes in response to and independent of (i.e. within the last 1,000 years) sea-level processes across the mid to late Holocene. Current models of reef island evolution from the Indo-Pacific have shown varying stages of sea-level adjustment over the Holocene. These include reef island formation: during a fall in relative sea level (e.g. Warrabar Island, Torres Strait; Woodroffe et al., 2007), post a fall in relative sea level (e.g. Mba Island, New Caledonia; Yamano et al., 2014), during the Holocene highstand (e.g. Cocos [Keeling] Islands; Woodroffe et al., 1999), during a rise in relative sea level (i.e. Holocene transgression; e.g. South Maalhosmadulu Atoll, Maldives; Kench

et al., 2005) or during present-day sea level (e.g. Tepuka Island, Tuvalu; Kench et al., 2014). The model of evolution for Eva Island is unique when compared to its global counterparts in that island development is sustained over both sea-level fall (i.e. 4,800–1,000 cal yr BP) and during stabilised sea levels (i.e. within the last 1,000 years from which sea levels have shown no further reduction). This is supported by: (1) the heterogenous age structure of island sediments, suggesting sustained accumulation, with on-going production and delivery to the landmass, (2) homogenous composition of sediments (mollusc/coral rich), which may reflect little to no change in historical reef ecology over time (despite sea-level fall and reduction in accommodation space), thus resulting in sustained carbonate production and supply, and (3) the continual delivery of sediments to the island landmass via possible intermittent high energy pulse events (i.e. tropical cyclone activity), which have been widely reported across the Pilbara region (Nott, 2011). Significantly, under stable sea-level conditions, there is evidence of planform readjustment that may be the result of changing metocean conditions (i.e. within climate windows across the mid to late Holocene), which occur independently of sea-level fluctuations. These results suggest that Eva Island, and more generally islands within the region, are highly

sensitive to changes in metocean conditions, due to their role in island accretion.

5.7 | Eva Island development in the context of carbonate production within turbid-water reef settings

Previous studies have highlighted the importance of sustained carbonate sediment supply in the nourishment of low-lying reef islands (Perry et al., 2011). Sediment supply is determined, in part, by local metocean boundary conditions (e.g. wind/wave climate) but also sediment production rates (i.e. skeletal remains of reef calcifiers and/or reconstituted relict framework material; Browne et al., 2021). Quantifying sediment production in reefal systems is complex, but particularly difficult in turbid-water (and remote) systems due to the fieldwork conditions (Zweifler et al., 2021). While numerous studies have highlighted lower carbonate sediment production rates on turbid-water reefs than clear-water reefs (Mallela, 2007; Mallela & Perry, 2007), there is also evidence that turbid reefs may exhibit sustained or higher carbonate sediment production, with comparable proportions of key *in-situ* and direct sediment producers. For example, a study by Browne (2011) on two inshore turbid reefs on the central Great Barrier Reef (Paluma Shoals and Middle Reef) reported a high proportion of mollusc (*ca* 25%) and coral (*ca* 32%) skeletal fragments within the sediment record. Interestingly, the composition of sediment constituents (>60 samples) was relatively uniform both within and between reefs, as such, it was proposed that this mix of constituents could represent a sediment signature for turbid coral reefs. Here, comparable proportions of molluscs (34%) and corals (27%–31%) were observed in the surficial sediments at Eva Island (Bonesso et al., 2022), and in the Holocene sediment record. The temporal stability of sediment constituents suggests that the carbonate factory (i.e. the reef) has not experienced any major shifts in reef ecology due to significant environmental changes and that these reefs have been consistently turbid over the course of island building. In addition, recent assessments of *in-situ* coral carbonate framework production for Eva Island (3.8 kg/m^2/year; see Dee et al., 2020), using the census-based carbonate budget methodology (see review by Browne et al., 2021), are comparable to many clear-water reef localities globally, reinforcing that turbid-water systems may support stable and productive carbonate factories. These results may have significant implications for clear-water systems which transition towards more turbid environments, whereby clear-water systems with turbid-tolerant calcifying communities (both molluscs and corals that are adapted to high sediment loads) may exhibit sustained island sediment budgets and therefore, heighten the resilience of these systems.

6 | CONCLUSION

This study highlights a unique record of reef island evolution within a turbid-water coral reef province within the Indo-Pacific. Results highlight that island formation is linked to incremental sea-level fall following the Holocene highstand, but more notably, under stable sea-level trajectories, probably attributed to variation and frequency in metocean boundary conditions over the last 2,000 cal yr BP. The heterogenous ages of island sediments along with homogenous sediment composition constituting mollusc and coral-rich sediments is suggestive of sustained island building processes (production and accumulation) over Eva′s accretionary evolution. Yet, these result highlight that reef island evolution is complex and site-dependant and may be influenced by local metocean factors (wind, wave, current and high energy event exposure), particularly during stabilised sea-level trajectories. Underpinning these temporal and spatial differences in island building is fundamental in evaluating susceptibility to future sea-level change and to better inform on future trajectories of reef island landforms under global environmental change scenarios, including declines in water quality conditions.

CONFLICT OF INTEREST STATEMENT

The authors declare there to be no competing financial or intellectual interests that could have influenced the scientific outputs reported in this publication.

DATA AVAILABILITY STATEMENT

The data that support the findings of this study are available in the supplementary material of this article.

ORCID

Joshua L. Bonesso 🆔 https://orcid.org/0000-0001-9191-0453
Caroline C. Mather 🆔 https://orcid.org/0000-0003-0920-0642

REFERENCES

Blott, S.J. & Pye, K. (2001) GRADISTAT: a grain size distribution and statistics package for the analysis of unconsolidated sediments. *Earth Surface Processes and Landforms*, 26(11), 1237–1248.

Bonesso, J.L., Browne, N.K., Murley, M., Dee, S., Cuttler, M.V., Paumard, V., Benson, D. & O'Leary, M. (2022) Reef to Island sediment connections within an inshore turbid reef Island system of the eastern Indian Ocean. *Sedimentary Geology*, 436, 106177.

Bonesso, J.L., Cuttler, M.V., Browne, N., Hacker, J. & O'Leary, M. (2020) Assessing Reef Island sensitivity based on LiDAR-derived morphometric indicators. *Remote Sensing*, 12(18), 3033.

Browne, N.K. (2011) Carbonate and terrigenous sediment budgets for inshore turbid reefs on the Great Barrier Reef. Ph.D. thesis, James Cook University, Townsville, Qld, Australia, pp. 83–84.

Browne, N.K., Cuttler, M., Moon, K., Morgan, K., Ross, C.L., Castro-Sanguino, C., Kennedy, E., Harris, D., Barnes, P. & Bauman, A. (2021) Predicting responses of geo-ecological carbonate reef systems to climate change: a conceptual model and review. *Oceanography and Marine Biology: An Annual Review*, 59(59), 229–370.

Cacciapaglia, C. & van Woesik, R. (2015) Climate-change refugia: shading reef corals by turbidity. *Global Change Biology*, 22(3), 1145–1154.

Callow, J.N., May, S.M. & Leopold, M. (2018) Drone photogrammetry and KMeans point cloud filtering to create high resolution topographic and inundation models of coastal sediment archives. *Earth Surface Processes and Landforms*, 43(12), 2603–2615.

Cartwright, P.J., Fearns, P.R., Branson, P., Cuttler, M.V., Oleary, M., Browne, N.K. & Lowe, R.J. (2021) Identifying metocean drivers of turbidity using 18 years of modis satellite data: implications for marine ecosystems under climate change. *Remote Sensing*, 13(18), 3616.

Collins, L.B., Zhao, J.X. & Freeman, H. (2006) A high-precision record of mid–late Holocene sea-level events from emergent coral pavements in the Houtman Abrolhos Islands, southwest Australia. *Quaternary International*, 145, 78–85.

Cuttler, M.V., Hansen, J.E., Lowe, R.J., Trotter, J.A. & McCulloch, M.T. (2019) Source and supply of sediment to a shoreline salient in a fringing reef environment. *Earth Surface Processes and Landforms*, 44(2), 552–564.

Cuttler, M.V.W., Vos, K., Branson, P., Hansen, J.E., O'Leary, M., Browne, N.K. & Lowe, R.J. (2020) Interannual response of reef islands to climate-driven variations in water level and wave climate. *Remote Sensing*, 12, 4089.

Dawson, J.L., Hua, Q. & Smithers, S. (2012) Benthic foraminifera: their importance to future reef island resilience. In: Proceedings, Twelfth International Coral Reef Symposium, Cairns, July 9–13 2012, Volume 1A: Reef and Reef Island Geomorphology.

Dee, S., Cuttler, M., O'Leary, M., Hacker, J. & Browne, N. (2020) The complexity of calculating an accurate carbonate budget. *Coral Reefs*, 39, 1–10.

Dickinson, W.R. (2009) Pacific atoll living: how long already and until when. *GSA Today*, 19(3), 4–10.

Dufois, F., Lowe, R.J., Branson, P. & Fearns, P. (2017) Tropical cyclone-driven sediment dynamics over the Australian North West Shelf. *Journal of Geophysical Research: Oceans*, 122, 10225–10244.

East, H.K., Perry, C.T., Kench, P.S., Liang, Y. & Gulliver, P. (2018) Coral reef Island initiation and development under higher than present sea levels. *Geophysical Research Letters*, 45(20), 11–265.

Ford, M.R., Kench, P.S., Owen, S.D. & Hua, Q. (2020) Active sediment generation on coral reef flats contributes to recent reef Island expansion. *Geophysical Research Letters*, 47(23), e2020GL088752.

Gourlay, M. (1988) Coral cays: products of wave action and geological processes in a biogenic environment. Proceedings of the 6th International Coral Reef Symposium Great Barrier Reef Committee Townsville, pp. 491–496.

Heaton, T.J., Köhler, P., Butzin, M., Bard, E., Reimer, R.W., Austin, W.E., Ramsey, C.B., Grootes, P.M., Hughen, K.A., Kromer, B. & Reimer, P.J. (2020) Marine20—the marine radiocarbon age calibration curve (0–55,000 cal BP). *Radiocarbon*, 62(4), 779–820.

Heery, E.C., Hoeksema, B.W., Browne, N.K., Reimer, J.D., Ang, P.O., Huang, D., Friess, D.A., Chou, L.M., Loke, L.H., Saksena-Taylor, P. & Alsagoff, N. (2018) Urban coral reefs: degradation and resilience of hard coral assemblages in coastal cities of East and Southeast Asia. *Marine Pollution Bulletin*, 135, 654–681.

Kench, P., Owen, S., Resture, A., Ford, M., Trevor, D., Fowler, S. & Langrine, J. (2011) Improving understanding of local-scale vulnerability in Atoll Island countries: developing capacity to improve in-country approaches and research. Final Report to the Asia-Pacific Network for Global Change Research.

Kench, P.S., McLean, R.F. & Nichol, S.L. (2005) New model of reef-Island evolution: Maldives, Indian Ocean. *Geology*, 33(2), 145–148.

Kench, P.S., Owen, S.D., Beetham, E.P., Mann, T., Mclean, R.F. & Ashton, A. (2020) Holocene sea level dynamics drive formation of a large atoll Island in the central Indian Ocean. *Global and Planetary Change*, 195, 103354.

Kench, P.S., Owen, S.D. & Ford, M.R. (2014) Evidence for coral Island formation during rising sea level in the central Pacific Ocean. *Geophysical Research Letters*, 41(3), 820–827.

Kench, P.S., Smithers, S.G. & McLean, R.F. (2012) Rapid reef Island formation and stability over an emerging reef flat: Bewick Cay, northern Great Barrier Reef, Australia. *Geology*, 40(4), 347–350.

Liang, C.Y., Kench, P.S., Ford, M.R. & East, H.K. (2022) Lagoonal reef Island formation in Huvadhoo atoll, Maldives, highlights marked temporal variations in Island building across the archipelago. *Geomorphology*, 414, 108395.

Mallela, J. (2007) Coral reef encruster communities and carbonate production in cryptic and exposed coral reef habitats along a gradient of terrestrial disturbance. *Coral Reefs*, 26, 775–785.

Mallela, J. & Perry, C.T. (2007) Calcium carbonate budgets for two coral reefs affected by different terrestrial run off regimes, Rio Bueno, Jamaica. *Coral Reefs*, 26, 129–145.

May, S.M., Callow, J.N., Brill, D., Hoffmeister, D. & May, J.H. (2021) Revealing sediment transport pathways and geomorphic change in washover fans by combining drone-derived digital elevation models and single grain luminescence data. *Journal of Geophysical Research: Earth Surface*, 126(1), e2020JF005792.

May, S.M., Brill, D., Leopold, M., Callow, J.N., Engel, M., Scheffers, A., Opitz, S., Norpoth, M. & Brückner, H. (2017) Chronostratigraphy and geomorphology of washover fans in the Exmouth Gulf (NW Australia)–a record of tropical cyclone activity during the Late Holocene. *Quaternary Science Reviews*, 169, 65–84.

Nott, J. (2011) A 6000-year tropical cyclone record from Western Australia. *Quaternary Science Reviews*, 30(5–6), 713–722.

Perry, C.T., Kench, P.S., Smithers, S.G., Riegl, B., Yamano, H. & O'Leary, M.J. (2011) Implications of reef ecosystem change for the stability and maintenance of coral reef islands. *Global Change Biology*, 17, 3679–3696.

Ramsey, C.B. (1995) Radiocarbon calibration and analysis of stratigraphy: the OxCal program. *Radiocarbon*, 37, 425–430. https://doi.org/10.1017/s0033822200030903

Storlazzi, C.D., Gingerich, S.B., van Dongeren, A., Cheriton, O.M., Swarzenski, P.W., Quataert, E., Voss, C.I., Field, D.W., Annamalai, H., Piniak, G.A. & McCall, R. (2018) Most atolls will be uninhabitable by the mid-21st century because of sea-level rise exacerbating wave-driven flooding. *Science Advances*, 4(4), eaap9741.

Turney, C., Becerra-Valdivia, L., Sookdeo, A., Thomas, Z.A., Palmer, J., Haines, H.A., Haines, H.A., Cadd, H., Wacker, L., Baker, A., Andersen, M.S., Jacobsen, G., Meredith, K., Chinu, K., Bollhalder, S. & Marjo, C. (2021) Radiocarbon protocols and first intercomparison results from the Chronos [14]carbon-cycle facility, University of New South Wales, Sydney, Australia. *Radiocarbon*, 63(3), 1003–1023.

Twiggs, E.J. & Collins, L.B. (2010) Development and demise of a fringing coral reef during Holocene environmental change, eastern Ningaloo Reef, Western Australia. *Marine Geology*, 275(1–4), 20–36.

Vousdoukas, M.I., Velegrakis, A.F. & Plomaritis, T.A. (2007) Beachrock occurrence, characteristics, formation mechanisms and impacts. *Earth-Science Reviews*, 85(1–2), 23–46.

Wacker, L., Bonani, G., Friedrich, M., Hajdas, I., Kromer, B., Němec, M., Ruff, M., Suter, M., Synal, H.A. & Vockenhuber, C. (2010) MICADAS: routine and high-precision radiocarbon dating. *Radiocarbon*, 52(2), 252–262.

Woodroffe, C.D., McLean, R.F., Smithers, S.G. & Lawson, E.M. (1999) Atoll reef-Island formation and response to sea-level change: West Island, Cocos (Keeling) Islands. *Marine Geology*, 160(1–2), 85–104.

Woodroffe, C.D. & Morrison, R.J. (2001) Reef-Island accretion and soil development on Makin, Kiribati, central Pacific. *Catena*, 44(4), 245–261.

Woodroffe, C.D., Samosorn, B., Hua, Q. & Hart, D.E. (2007) Incremental accretion of a sandy reef Island over the past 3000 years indicated by component-specific radiocarbon dating. *Geophysical Research Letters*, 34(3), 1–5.

Woodroffe, C. (1992) Mangrove sediments and geomorphology. *Tropical Mangrove Ecosystems*, 41, 7–41.

Wu, M., Duvat, V.K. & Purkis, S.J. (2021a) Multi-decadal atoll-Island dynamics in the Indian Ocean Chagos Archipelago. *Global and Planetary Change*, 202, 103519.

Wu, M., Harris, P.M., Eberli, G. & Purkis, S.J. (2021b) Sea-level, storms, and sedimentation–controls on the architecture of the Andros tidal flats (Great Bahama Bank). *Sedimentary Geology*, 420, 105932.

Yamano, H., Cabioch, G., Chevillon, C. & Join, J.L. (2014) Late Holocene sea-level change and reef-Island evolution in New Caledonia. *Geomorphology*, 222, 39–45.

Yamano, H., Miyajima, T. & Koike, I. (2000) Importance of foraminifera for the formation and maintenance of a coral sand cay: Green Island, Australia. *Coral Reefs*, 19, 51–58.

Zweifler, A., Oleary, M., Morgan, K. & Browne, N.K. (2021) Turbid coral reefs: past, present and future—a review. *Diversity*, 13, 251.

SUPPORTING INFORMATION

Additional supporting information can be found online in the Supporting Information section at the end of this article.